Dalton Transactions

Cooperative Bimetallic Reactivity of a Heterodinuclear Molybdenum-Copper Model of Mo-Cu CODH

Journal:	*Dalton Transactions*
Manuscript ID	DT-ART-06-2018-002323.R1
Article Type:	Paper
Date Submitted by the Author:	18-Jun-2018
Complete List of Authors:	Groysman, Stanislav; Wayne State University, Chemistry Hollingsworth, Thilini; Wayne State University, Chemistry Hollingsworth, Ryan; Wayne State University, Chemistry Lord, Richard; Grand Valley State University, Chemistry

Journal Name

ARTICLE

Cooperative Bimetallic Reactivity of a Heterodinuclear Molybdenum-Copper Model of Mo-Cu CODH

Received 00th January 20xx,
Accepted 00th January 20xx

DOI: 10.1039/x0xx00000x

www.rsc.org/

Thilini S. Hollingsworth,[a] Ryan L. Hollingsworth,[a] Richard L. Lord,[b] and Stanislav Groysman[a]*

The synthesis of a heterodinucleating ligand LH_2 (LH_2 = (E)-3-(((2,7-di-tert-butyl-9,9-dimethyl-5-((pyridin-2-ylmethylene)amino)-9H-xanthen-4-yl)amino)methyl)benzene-1,2-diol) was undertaken toward a functional model of the bimetallic active site found in Mo-Cu carbon monoxide dehydrogenase (Mo-Cu CODH), and to understand the origins of heterobimetallic cooperativity exhibited by the enzyme. LH_2 features a hard potentially dianionic catechol chelate for binding Mo(VI) and a soft iminopyridine chelate for binding Cu(I). Treatment of LH_2 with either Cu(I) or M(VI) (M = Mo, W) sources leads to the anticipated site-selective incorporation of the respective metals. While both $[Cu^{I}(LH_2)]^{+}$ and $[M^{VI}O_3(L)]^{2-}$ complexes are stable in the solid state, $[M^{VI}O_3(L)]^{2-}$ complexes disproportionate in solution to give $[M^{VI}O_2(L)_2](NEt_4)_2$ complexes, with $[M^{VI}O_4]^{2-}$ as the by-product. The incorporation of BOTH Mo(VI) and Cu(I) into L forms a highly reactive heterobimetallic complex $[Mo^{VI}O_3Cu^{I}(L)](NEt_4)_2$, whose formation and reactivity was interrogated via ^{1}H NMR/UV-vis spectroscopy and DFT calculations. These studies reveal that the combination of the two metals triggers oxidation reactivity, in which a nucleophilic Mo(VI) trioxo attacks Cu(I)-bound imine. The major product of the reaction is a crystallographically characterized molybdenum(VI) complex $[Mo(L^*)O_2](NEt_4)$ coordinated by a modified ligand L* that contains a new C-O bond in place of the imine functionality. This observed hydroxylation reactivity is consistent with the postulated first step of Mo-Cu CODH (nucleophilic attack of the Mo(VI)-oxo on the Cu(I)-bound electrophilic CO) and Xanthine Oxidoreductase (nucleophilic attack of Mo(VI)-oxo on the electrophilic xanthine carbon).

Introduction

There is a significant current interest in the design of heterodinuclear complexes for cooperative bimetallic reactivity in small molecule activation and catalysis.[1] This interest originates in recent discoveries of bimetallic and multimetallic sites in nature that catalyze efficiently difficult multielectron transformations, such as dinitrogen and carbon dioxide reduction.[2] Molybdenum-copper carbon monoxide dehydrogenase (Mo-Cu CODH) catalyzes reversible oxidation of CO, according to the following equation: $CO + H_2O \leftrightarrow CO_2 + 2H^+ + 2e^-$.[3, 4] The active site of Mo-Cu CODH contains a molybdenum(VI) center linked to a copper(I) center through a sulfido bridge (Fig. 1).[3, 4] The molybdenum fragment closely resembles the active site of the xanthine oxidoreductase family (XOR, Fig. 1), in which molybdenum(VI) is ligated by a single pyranopterindithiolene cofactor, two oxo ligands, and one sulfide.[4, 5] The copper fragment contains low-coordinate copper(I) ligated by a cysteinate ligand, in addition to Mo-sulfido.[3, 6, 7] The mechanism of CO oxidation by the active site of Mo-Cu CODH is postulated to commence with CO coordination to the unsaturated copper(I) site, followed by an attack of a reactive basal molybdenum-oxo.[3, 7-11] The exact role of the bridging sulfido in the reaction mechanism is currently under debate. Earlier studies advocated both structural and functional roles, which involves a direct interaction (insertion) between CO and bridging sulfido.[3, 8, 9] More recently, Hille, Kirk and coworkers suggested that the bridging sulfido may play a primarily structural (or structural/electronic) role, bringing Cu-coordinated CO close to the reactive Mo-oxo.[7, 11] Overall, Mo-Cu CODH functions as an oxo-transferase, catalyzing oxo-transfer to CO. The related XOR is a hydroxylase, that formally inserts oxo into C-H bonds of hypoxanthine (to give xanthine) and xanthine (to give uric acid).[4, 5] In both cases, the molybdenum(VI)-oxo functionality is likely rendered sufficiently nucleophilic due to the presence of several multiply-bonded ligands at the metal. It is generally accepted that monooxo d^0 complexes (e. g. $Mo^{VI}O$) demonstrate an M-O bond order of 3, which leads to an electrophilic behavior at the oxo.[12-14] In contrast, complexes featuring two oxo groups (e. g. $Mo^{VI}O_2$) demonstrate lower M-O bond orders due to the lack of a sufficient number of dπ orbitals of the appropriate symmetry.[13, 15] Furthermore, in trioxo (or mixed oxo-sulfido variants) $Mo^{VI}O_3$ ($M^{VI}O_nS_{3-n}$) complexes and beyond, the bond

[a] Department of Chemistry, Wayne State University, 5101 Cass Ave, Detroit, MI, 48202, USA. E-mail: groysman@chem.wayne.edu
[b] Department of Chemistry, Grand Valley State University, Allendale, MI, 49401, USA. E-mail: lordri@gvsu.edu
Electronic Supplementary Information (ESI) available: Synthetic procedures, experimental data, and Cartesian coordinates. See DOI: 10.1039/x0xx00000x

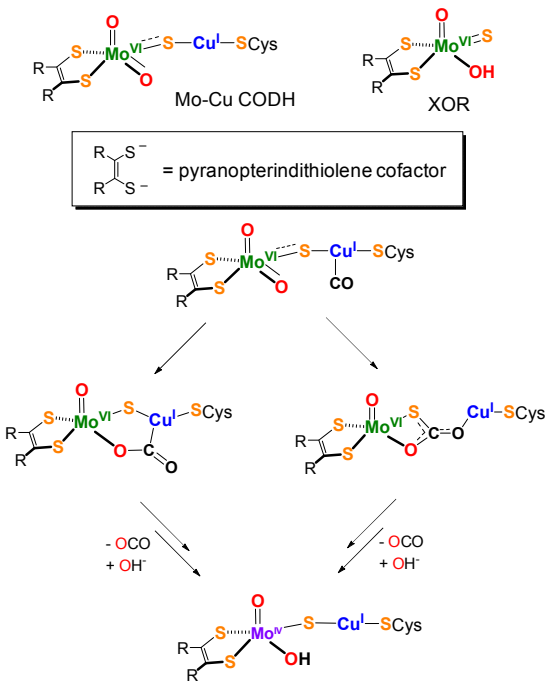

Fig. 1. Top: Active sites of Mo-Cu carbon monoxide dehydrogenase (CODH) and Xanthine Oxidoreductase (XOR). Bottom: possible CO oxidation mechanisms highlighting structural only (left) and structural/functional role of the bridging sulfide (right).

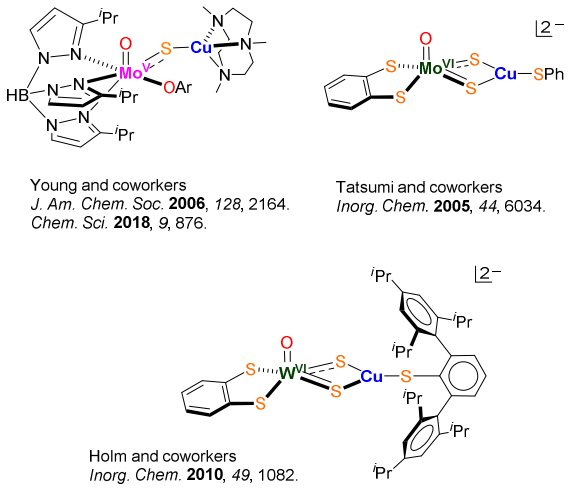

Fig. 2. Previously reported structural models of Mo-Cu CODH.

order of individual metal-oxo functions decrease significantly, which leads to nucleophilic reactivity.[16, 17] In both CODH and XOR, a nucleophilic molybdenum oxo attacks an electrophilic substrate: heterocyclic carbon in XOR and Cu(I)-bound CO in CODH.[4, 7]

The unprecedented structure of the Mo-Cu CODH active site prompted several research groups to pursue its biomimetic chemistry.[18-21] These efforts culminated in several structural models, capturing some of the structural features of the Mo-Cu CODH active site (Fig. 2). Young and coworkers reported a Mo(V)-Cu(I) complex bridged by a single sulfido, a disposition made possible by the coordinative saturation of both molybdenum and copper.[19] Holm and coworkers used their previously synthesized model of XOR, $[WO_2S(bdt)](NEt_4)_2$,[20 22] as a precursor for a reaction with low-coordinate Cu(I) complexes.[23] This reaction led to the formation of a disulfido bridge in $W^{VI}O_2(bdt)(\mu^2\text{-}S)_2Cu^{I}(SR)$. Molybdenum complexes of similar topology were previously reported by Tatsumi and coworkers.[21] We are unaware of any structural Mo-Cu CODH model that is capable of oxidation reactivity as well. We postulated that the use of a dinucleating ligand, capable of binding both molybdenum(VI) and copper(I), might increase the stability of the bimetallic system and enable reactivity studies. As we are not seeking the precise structural model, the [Mo-S-Cu] structural motif was not pursued in this study. As noted above, while the structural role of the bridging sulfido in bringing two reactive metals together is well established, its functional participation in CO oxidation is still debated.[7] In this manuscript, we describe a new heterodinucleating ligand, capable of selective binding of Cu(I) and Mo(VI)-oxo in close proximity. We report that while monometallic (either Cu(I) or Mo(VI)) complexes of the heterodinucleating ligand are relatively stable, coordination of both metals immediately triggers oxidation reactivity by the Mo(VI)-oxo. This is the first example where bimetallic cooperativity is observed for a model of Mo-Cu CODH.

Results and Discussion

In the design of our system, we targeted the following features that appear essential for the enzymatic reactivity: (i) placement of Cu(I) in the vicinity of Mo(VI); (ii) presence of several multiply bonded groups on Mo(VI); (iii) coordinative unsaturation of Cu(I). Our synthetic endeavours focused on the ligand LH_2 (Scheme 1). LH_2 combines a hard dianionic catechol (for Mo(VI) binding) with a soft iminopyridine (for Cu(I) binding) via the intermediacy of 2,7-di-tert-butyl-9,9-dimethyl-4,5-diaminoxanthene, that has been previously shown to serve as a suitable linker for dinucleating ligands.[24] Ligand synthesis involves an initial condensation of 2,3-dihydroxybenzaldehyde with 2,7-di-tert-butyl-9,9-dimethyl-xanthene-4,5-diamine, followed by a reduction with sodium borohydride. The condensation of the product with pyridine-2-carboxaldehyde yields LH_2. LH_2 has been obtained as a yellow solid and characterized by ^1H and ^{13}C NMR spectroscopy, high-resolution mass spectrometry, and elemental analysis.

To evaluate the selectivity of the binding positions of LH_2 for the designated metals, the reaction of LH_2 with a Cu(I) precursor, $[Cu(NCMe)_4](PF_6)$, was investigated first. In addition, we also interrogated the reactivity of $[Cu(NCMe)_4](B(C_6F_5)_4)$, as the latter counter-ion often exhibits better solubility and higher stability. Treatment of $[Cu(NCMe)_4](PF_6)$ with the THF solution of LH_2, led to the formation of $[Cu(LH_2)](PF_6)$ (**1**(PF_6)), isolated as a red-brown

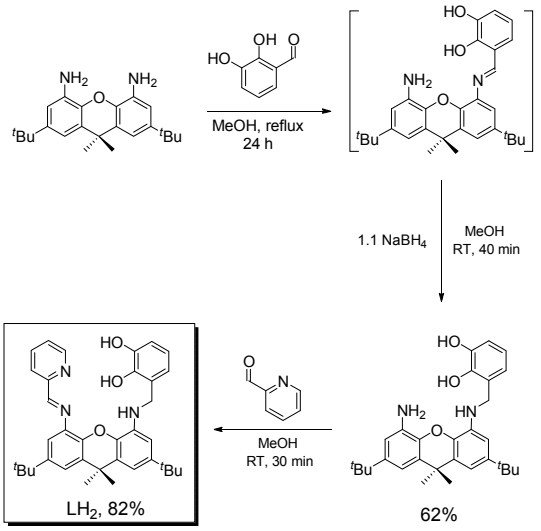

Scheme 1. Synthesis of LH_2.

crystalline solid in 94% yield. The ^{1}H NMR spectrum of **1**(PF_6) demonstrates slightly broadened resonances, particularly in the aromatic region. Catechol OH signals are observed as well, suggesting that copper(I) does not bind to the catecholate functionality. The ^{1}H NMR spectrum of $[Cu(LH_2)](B(C_6F_5)_4)$ (**1**($B(C_6F_5)_4$)) demonstrates overall similar, albeit sharpened, spectroscopic features. No difference in stability was observed between **1**(PF_6) and **1**($B(C_6F_5)_4$). ESI-MS (positive mode) for both **1**(PF_6) and **1**($B(C_6F_5)_4$) contain peaks corresponding to the molecular ion $[\mathbf{1}]^+$: m/z of 626.2438 (predicted 626.2438) for **1**($B(C_6F_5)_4$), and 626.2446 for **1**(PF_6) (see ESI). X-ray quality crystals of **1**(PF_6) were obtained by recrystallization from THF/ether. X-ray structure determination reveals tridentate coordination of LH_2 to copper(I), via all the nitrogens in the ligand (Fig. 3).‡ Selected bond lengths are given in Fig. 3. Copper(I) coordination to the secondary (benzylic) nitrogen rigidifies the overall structure and positions the catechol unit above copper-iminopyridine. The copper(I) site of Mo-Cu CODH exhibits the coordinative unsaturation necessary for the initial substrate binding. The copper(I) center in **1** is 3-coordinate, and thus should also be capable of binding an additional ligand. To demonstrate coordinative unsaturation of copper in **1**, we treated it with a CO analogue, isocyanide CN(2,6-Me_2Ph). As the reaction of **1**($B(C_6F_5)_4$) led to a better defined NMR spectra, we limited our studies to the $B(C_6F_5)_4$ salt. The addition of isocyanide to $[Cu(LH_2)](B(C_6F_5)_4)$ forms an isocyanide complex $[Cu(LH_2)(CN(2,6\text{-}Me_2Ph)](B(C_6F_5)_4)$ (**2**($B(C_6F_5)_4$), isolated as a red-orange solid in 96% yield. The coordination of isocyanide to copper(I) in **2**($B(C_6F_5)_4$) is established by NMR and IR spectroscopy. ^{1}H NMR spectrum (CD_2Cl_2) demonstrates a signal for the isocyanide Me groups at 2.26 ppm (2.41 ppm for free isocyanide). The IR signal for the CN stretch is found at 2145 cm^{-1} (2118 cm^{-1} for free isocyanide), as expected for an isocyanide ligand that binds primarily through σ-donation.

Following the determination of the copper(I) coordination mode to the ligand, we investigated the reactivity of LH_2 with

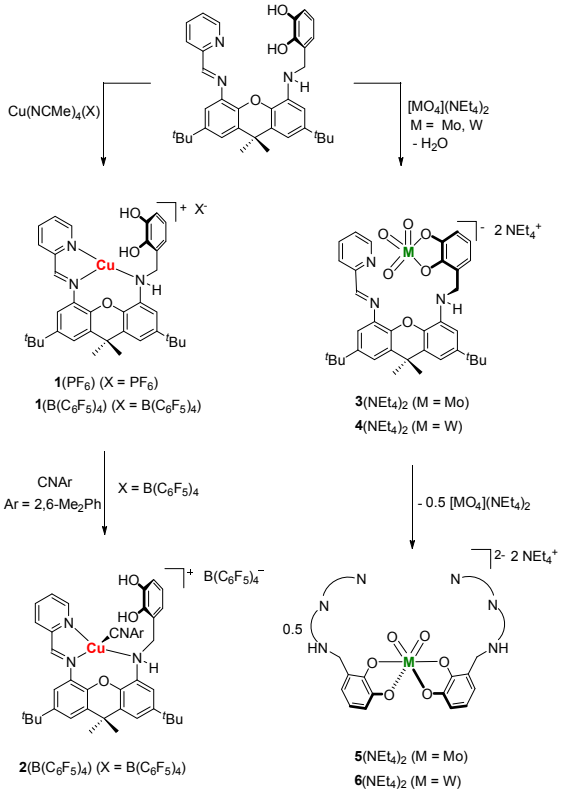

Scheme 2. Reactions of LH2 with Cu(I) and Mo(VI)/W(VI) precursors.

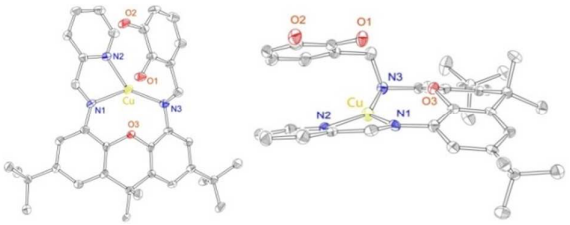

Fig. 3. X-ray structure of **1**(PF_6), 50% probability ellipsoids. PF_6 counter-ion and co-crystallized ether molecules are omitted for clarity. Selected bond distances (Å) and angles (°): Cu N1 2.151(3), Cu N2 2.010(3), Cu N3 2.011(3), N1 Cu N2 79.17(10), N2 Cu N3 144.2(1), N1 Cu N3 132.4(1).

molybdenum(VI). As tungsten(VI) is known to exhibit similar structural and functional chemistry, but is often more stable than its molybdenum(VI) counterpart,[25] its chemistry was also studied. Slow addition of the ligand precursor in THF to cold acetonitrile solutions of $[MO_4](NEt_4)_2$[26] (M = Mo(VI), W(VI)) forms complexes $[Mo(O_3)L](NEt_4)_2$ (**3**$(NEt_4)_2$) and $[W(O_3)L](NEt_4)_2$ (**4**$(NEt_4)_2$). Complexes **3**$(NEt_4)_2$ and **4**$(NEt_4)_2$ are isolated as yellow crystals by recrystallization of the crude product from THF/CH_3CN/ether. The nature of the complexes was established by ^{1}H and ^{13}C NMR spectroscopy, high-resolution mass spectrometry, and elemental analysis. The ^{1}H NMR spectrum demonstrates significant change in the chemical shifts of the catecholate aryl protons compared with the free ligand, suggesting catecholate coordination to molybdenum/tungsten. OH protons, previously observed in the spectra of the free ligand and **1**(PF_6), are notably absent in

the spectra of **3**$(NEt_4)_2$ and **4**$(NEt_4)_2$. Mass spectra for both compounds are consistent with the proposed formulations of **3**$(NEt_4)_2$ and **4**$(NEt_4)_2$ as depicted in Scheme 2, allowing the observation of the molecular ions (see ESI). We were not able to obtain solid-state structures of **3**$(NEt_4)_2$ and **4**$(NEt_4)_2$, due to the very thin nature of the crystals. We also note that the $[M^{VI}O_3(catecholate)]$ is a rare structural motif in the chemistry of Mo and W, presumably due to the nucleophilicity of the trioxo functionality (see below). A CCDC search revealed only one structure containing $[Mo^{VI}O_3(catecholate)]$,[27] and no respective W structures, as opposed to ~40 structures of $MoO_2(catecholate)_2$ and ~20 $WO_2(catecholate)_2$ complexes.

3$(NEt_4)_2$ and **4**$(NEt_4)_2$ are stable indefinitely in solid state. In solution, however, both complexes undergo disproportionation to give $[M(O_2)L_2](NEt_4)_2$ complexes **5**$(NEt_4)_2$ (M = Mo) and **6**$(NEt_4)_2$ (M = W) and $[MO_4](NEt_4)_2$. The reaction is relatively slow in solvents of low polarity, dichloromethane and THF. Thus, a CD_2Cl_2 solution of **3**$(NEt_4)_2$ (0.02 M molarity) demonstrates about 30% of **5**$(NEt_4)_2$ after 24 hours at room temperature. The more polar solvent acetonitrile leads to a significantly faster transformation of **3**$(NEt_4)_2$ to **5**$(NEt_4)_2$, which is complete within 3 hours. Complexes **5**$(NEt_4)_2$ and **6**$(NEt_4)_2$ can also be synthesized directly by treating $[MO_4](NEt_4)_2$ with two equivalents of LH_2. **5**$(NEt_4)_2$ and **6**$(NEt_4)_2$ are characterized by ^1H and ^{13}C NMR spectroscopy, mass spectrometry, and elemental analyses. There are several notable differences between the NMR spectra of **5**$(NEt_4)_2$/**6**$(NEt_4)_2$ and of **3**$(NEt_4)_2$/**4**$(NEt_4)_2$. Most importantly, whereas **3**$(NEt_4)_2$/**4**$(NEt_4)_2$ appear as single species in their ^1H spectra, several species are observed in the spectra of **5**$(NEt_4)_2$/**6**$(NEt_4)_2$. We hypothesized that the observation of several species is due to the presence of several conformers most likely involving bond rotation within L. VT NMR supported this hypothesis: heating the sample to 50 ºC leads to peak coalescence and the observation of single species for **6**$(NEt_4)_2$ (see ESI). We were able to obtain X-ray structure of **6**$(NEt_4)_2$ (Fig. 4), that confirmed expected catecholate coordination to the metal, and provided additional support for the proposed structures of complexes **3**$(NEt_4)_2$ and **4**$(NEt_4)_2$. Second coordination site, containing three nitrogens, is not bound to the metal. The geometry around W(VI) center in **6** is distorted octahedral. It should be also noted that **6** features crystallographic C_2 symmetry, giving rise to one distinct W-oxo bond distance, and two W-catecholate bonds distances (Fig. 4).

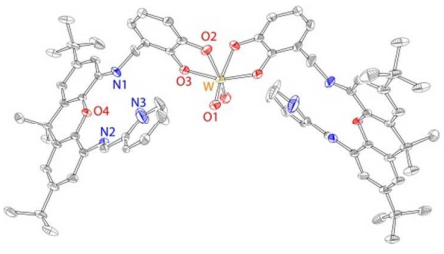

Fig. 4. X-ray structure of **6**$(NEt_4)_2$, 40% probability ellipsoids. NEt_4 counter-ions are omitted for clarity. Selected bond distances (Å): W O1 1.747(6), W O2 2.122(5), W O3 2.009(4).

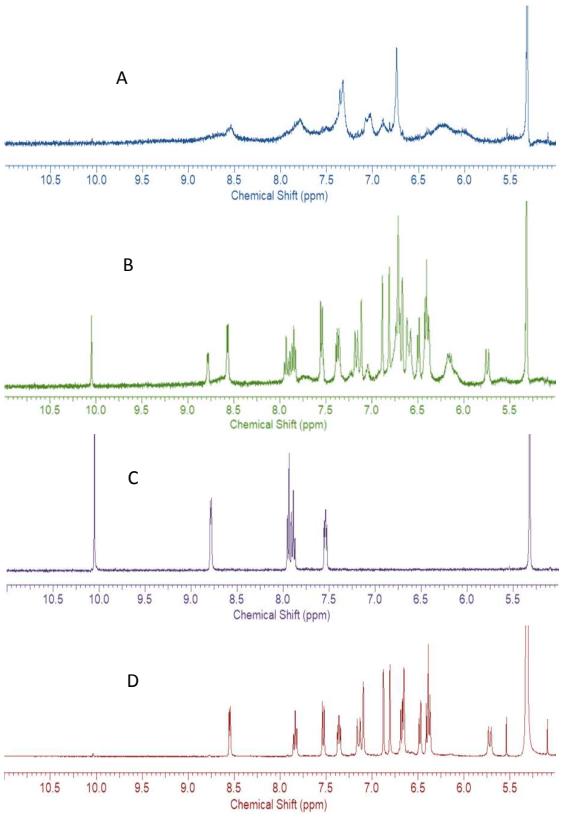

Fig. 5. **A**: NMR spectrum obtained immediately after the addition of molybdate to the solution of **1**(PF_6). **B**: NMR spectrum of the same solution collected after 45 h. **C**: NMR spectrum of pure pyridine-2-carboxaldehyde. **D**: NMR spectrum of crystallized **7**. All spectra were collected in CD_2Cl_2; only the 5-11 ppm region is shown.

Having established the coordination modes of L with Mo(VI)/W(VI) and Cu(I) separately, we turned to the synthesis of heterobimetallic complexes. Addition of red-brown **1**(PF_6) or **1**$(B(C_6F_5)_4)$ to the colorless solutions of $[MoO_4](NEt_4)_2$ leads to formation of brown solution. ^1H NMR of the product mixture (Fig. 5, A) demonstrates broad resonances, from which no indication on the nature of the resulting species can be obtained. The addition of $[Cu(NCMe)_4](PF_6)$ to the solutions of **3**$(NEt_4)_2$ and **4**$(NEt_4)_2$ leads to similar color changes and similarly uninformative NMR spectra. The addition of $[Cu(NCMe)_4](PF_6)$ to the CH_2Cl_2 solution of **4**$(NEt_4)_2$ was followed by UV-vis spectroscopy (ESI). The UV-vis spectra reveal a slight shift in an "isosbestic" point throughout the addition, suggesting that the initial formation of heterobimetallic complexes may be followed by another reaction. However, it could also result from concentration changes, due to different solubilities of products vs. reactants. To shed light on the nature of the final product(s), we monitored the crude reaction mixture, resulting from the addition of $[MoO_4](NEt_4)_2$ to **1**(PF_6), by ^1H NMR spectroscopy over several days. ^1H NMR spectrum obtained after approximately 45 h (Fig. 5, B) differed significantly from the initial spectrum. The aromatic region indicated the presence of ~3 species. Comparison of the obtained spectrum with the spectrum of pyridine-2-carboxaldehyde (Fig. 5, C), indicated

that one of the species formed is pyridine-2-carboxaldehyde. Recrystallization of the product mixture (CD_2Cl_2, -30 °C), led to isolation of the major product (**7**(NEt_4)), obtained as yellow crystals. **7**(NEt_4) was characterized by X-ray crystallography, NMR spectroscopy, and HRMS. The structure of **7**(NEt_4) (Fig. 6) reveals an anionic molybdenum(VI) complex [Mo(L')O_2](NEt_4) coordinated by a modified L ligand (L') that contains a new C-O bond in place of the imine functionality; the imine is transformed into a secondary amine. L' binds to the metal via catecholate and alkoxy-pyridine; the remaining two positions at molybdenum are occupied by *cis* oxo groups. The high-resolution mass spectrum of **7**(NEt_4) demonstrates a molecular ion peak at m/z = 708.1968 (m/z of 708.1977 calculated for $[Mo(L')O_2]^-$). The NMR spectrum of **7**(NEt_4) is consistent with its solid-state structure (Fig. 5, D). Thus, instead of the previously observed imino proton, a doublet at 5.74 ppm is observed, consistent with the alkoxo methine sandwiched between NH and pyridine. The neighbouring N*H* signal (correlated to the alkoxo C*H* by COSY) appears as a doublet at 7.17 ppm. Full assignment of the spectrum is given in the ESI.

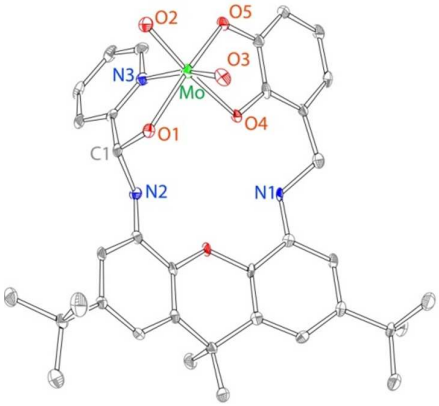

Fig. 6. X-ray structure of **7**(NEt_2), 40% probability ellipsoids. NEt_4 counter-ions are omitted for clarity. Selected bond distances (Å): Mo O1 2.1449(2), Mo O2 1.7119(2), Mo O3 1.7105(2), Mo O4 1.9870(2), Mo O5 1.9230(2), Mo N3 2.352(2).

Matching the proton spectrum of pure **7**(NEt_4) (Fig. 5, D) with the spectrum of the product mixture (Fig. 6, B) confirms that **7**(NEt_4) is a major product. In addition to **7**(NEt_4) and pyridine-2-carboxaldehyde, the spectrum of the product mixture contains broad peaks which can be attributed to an additional by-product of the reaction, tentatively assigned here as "**8**(NEt_4)". It is hypothesized that "**8**(NEt_4)" is a molybdenum(VI) complex with the fully hydrolyzed imine. A possible structure of "**8**(NEt_4)" is given in Scheme 3; however, it is also possible that "**8**(NEt_4)" is a dimer, which may explain its broad NMR signals. The ratio between different reaction products is temperature-dependent. The product ratio does not change significantly after ~ 48 hours at room temperature. In contrast, storing the reaction mixture at -30 °C for seven days leads mostly to the formation of compound **7**(NEt_4), at the expense of pyridine-2-carboxaldehyde and "**8**(NEt_4)". After two weeks, the spectrum contains only compound **7**(NEt_4) (obtained in 95%). This information, supported by DFT calculations (see below) led us to propose a reaction mechanism. Based on the reactions of L with copper(I) and molybdenum(VI)/tungsten(VI) described above, we postulate initial formation of a Mo/Cu heterodinuclear complex "**9**(NEt_4)", accompanied by the formation of water. Next, a nucleophilic molybdenum oxo attacks the electrophilic imino carbon, that is positioned close to and activated by coordination to copper(I), to form a molybdenum(VI)-alkoxo and anionic amido. We note that the nucleophilic attack of the Mo(VI)-oxo on the Cu-coordinated (electrophilic) substrate is consistent with the Mo-Cu CODH computational mechanism recently proposed by Kirk and coworkers.[11] The anionic amido is protonated by water, which may remain coordinated directly to Mo, or via H-bonds to catechol/amine/oxo functions. The copper(I) is lost, possibly due to amido protonation, or due to the induced flexibility of the [NNN] chelate, which enables pyridine coordination to Mo(VI). The immediate hydroxylation product, **7**(NEt_4), exists in the temperature-dependent equilibrium with "**8**(NEt_4)" and pyridine-2-carboxaldehyde.

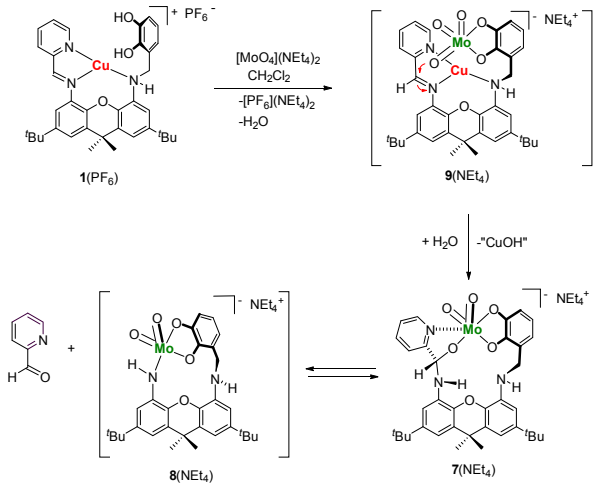

Scheme 3. Possible mechanism for the formation of **7**, pyridine-2-carboxaldehyde and "**8**" via postulated bimetallic intermediate "**9**".

Is there any evidence for a cooperative bimetallic effect in our system, where the presence of copper(I) facilitates hydroxylation? To answer this question, we monitored the CD_2Cl_2 solution of [Mo(L)O_2](NEt_4)$_2$ (**3**(NEt_4)$_2$) by ^{1}H NMR spectroscopy for several days. As noted above, CD_2Cl_2 solution of [Mo(L)O_2](NEt_4)$_2$ undergoes slow decomposition into [Mo(L)$_2$$O_2$]($NEt_4$)$_2$ (**5**(NEt_4)$_2$). NMR indicates that after 3 days, approximately 85% of the materials consists of **3**(NEt_4)$_2$ and of **5**(NEt_4)$_2$. Only traces of pyridine-2-carboxaldehyde and **7**(NEt_4) are observed in ^{1}H NMR spectrum. To better understand the role of copper(I) in this hydroxylation, we turned to DFT calculations (see ESI for computational details).

Geometry optimization of the hypothetical intermediate **9** resulted in a well-defined minimum that has the MoO_3 moiety situated above the Cu-iminopyridine plane, as demonstrated in Fig. 7 (top left) and similar to the experimental structure for **1**. Nucleophilic attack on the imine by the Mo-oxo group in **9** to form **10** (Fig. 7, bottom left), the intermediate formed prior to

water exposure that makes "CuOH" and **7**, is calculated to be slightly endergonic by 2.5 kcal/mol. Importantly, the free energy barrier for this nucleophilic attack is only slightly higher at 4.6 kcal/mol. This suggests that nucleophilic attack of the imine when Cu(I) is bound in this bimetallic framework should be thermodynamically and kinetically accessible, consistent with the proposed mechanism (Fig. 6).

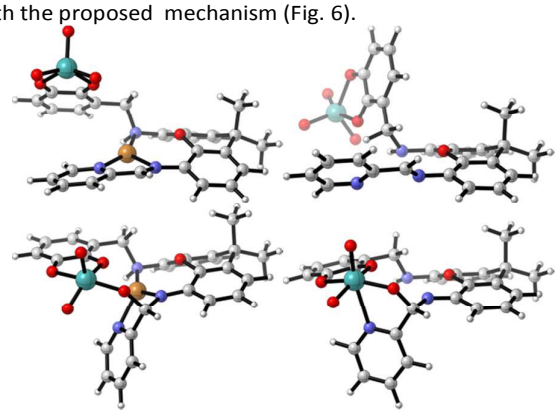

Fig. 7. Geometry optimized structures of **9** (top left), **3** (top right), **10** (bottom left), and **11** (bottom right).

To understand the cooperative bimetallic effect, we also investigated nucleophilic attack on the imine in **3**. Geometry optimization of **3**, despite having an input structure similar to that of **1** and **9**, results in the aminocatechol arm of the ligand swinging away from the iminopyridine (Fig. 7, top right). One cooperative effect is that coordination of the aminocatechol amine to Cu(I) prevents such rotations from taking place in **9**. However, given the relatively free rotation between the amine and the xanthene backbone, this should not prevent nucleophilic attack of the imine. An analogous product to **10**, except with Cu(I) removed, was also optimized (**11**, Fig. 7 bottom right). The structure of **11** is similar to **10** except that pyridine coordinates to Mo(VI) upon nucleophilic attack, and this intermediate much more endergonic at 16.3 kcal/mol. The free energy barrier is also much higher at 25.7 kcal/mol. There is a clear cooperative energetic effect in addition to the structural pre-disposition in **9** vs. **3** toward imine reactivity. To understand the origin of this energetic cooperativity, the frontier orbitals of **3** and **9** were analyzed (Fig. 8). The LUMO in both complexes is an iminopyridine π* orbital. Cu(I) coordination stabilizes this orbital by 0.76 eV. The relevant donor orbital with Mo-oxo character, the HOMO-2 in both complexes, is only stabilized by 0.28 eV because the Cu(I) ion does not directly interact with the Mo-oxo moiety. Thus, the better orbital energy matching when Cu(I) is bound (ΔE_{orb} = 1.01 eV) vs. when it is not (ΔE_{orb} = 1.49 eV) leads to a stronger nucleophile/electrophile interaction that lowers the energy barrier and endergonicity of the nucleophilic attack intermediate. Analogous trends were observed for W(VI) containing species (see Supporting Information).

Notably, the observed hydroxylation reactivity is also reminiscent of the reactivity of Xanthine Oxidoreductase (XOR). The proposed mechanism of XOR is given in Scheme 4.[23]

The reaction is initiated by deprotonation of the basal hydroxo[24] to create a nucleophilic basal oxo that is part of the [$Mo^{VI}O_2S$] active site. The key step is the nucleophilic attack of

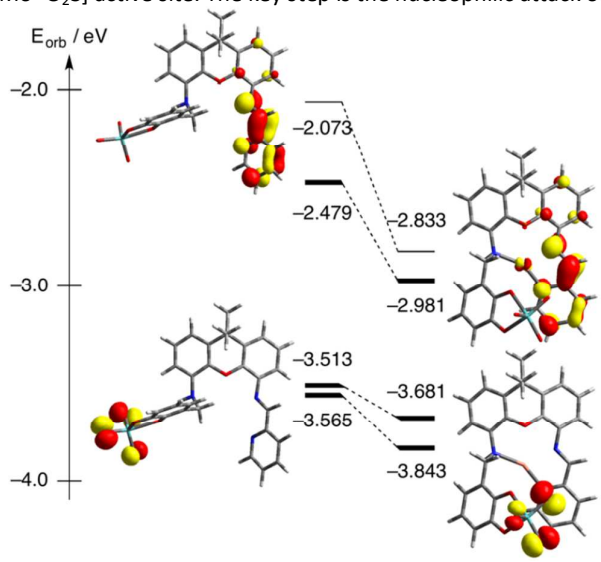

Fig. 8 Frontier orbital diagrams for **3** (left) and **9** (right) showing the LUMO and HOMO–2 orbitals involved in the nucleophile/electrophile interaction. Bond lines correspond to doubly occupied orbitals, while regular lines correspond to unoccupied orbitals. Orbital isosurfaces are plotted at 0.05 au.

the basal molybdenum-oxo to form a new C-O bond at the C8 position of xanthine, which is followed by a hydride transfer to the Mo^{VI}-sulfido. In our system, a nucleophilic basal Mo^{VI}-oxo attacks the electrophilic (imino) carbon to form a new C-O bond, which parallels the nucleophilic attack on C8 position in xanthine oxidation. The postulated roles of the second metal in Mo-Cu CODH, positioning and activation of the substrate towards nucleophilic attack, are played by H-bonding and electrostatic interactions in the active site pocket of XOR (not shown in Scheme 4).[4, 5] The nucleophilic attack and hydride transfer are postulated to proceed in one step in the enzymatic mechanism of XOR. Our system demonstrates only the nucleophilic attack because it lacks a suitable hydride acceptor. In our future studies, we will investigate the reactivity of our system in the presence of a hydride acceptor, and will also attempt to replace the imine with imidazole.

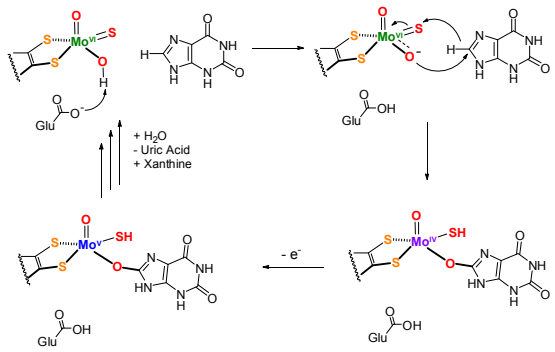

Scheme 4. Key steps in the mechanism of XOR.

Summary and Conclusions

In summary, we reported a new approach toward a functional model of Mo-Cu CODH, where the heterobimetallic site is assembled with an aid of heterodinucleating ligand. The ligand shows preferential binding of the metals in the designated positions: catecholate binds Mo(VI)/W(VI) trioxo, whereas the iminopyridine-amine binds Cu(I). Coordination of both metals triggers reactivity: a highly nucleophilic basal Mo(VI)-oxo function attacks electrophilic Cu(I)-coordinated imine. In the absence of Cu(I), only traces of hydroxylation products are observed. Thus, this study demonstrates cooperative bimetallic reactivity between Mo(VI) and Cu(I), suggesting that Cu(I) (in Mo-Cu CODH) may play a role in: (1) bringing the substrate to the vicinity of nucleophilic molybdenum-oxo; (2) ensuring the electrophilic character of the CO carbon. The present study also emphasizes the reactive nature of $[Mo^{VI}O_nS_{3-n}]$ (n = 0, 1) functional group that carries out the nucleophilic attack in both Mo-Cu CODH and XOR. Our work suggests that the first step in the reaction mechanism (nucleophilic attack) is possible without the presence of the bridging/terminal sulfido. It is not clear however whether the sulfido (or related redox-active functionality linking the product to Mo) is necessary for the electron transfer to Mo. Our future studies will focus on related heterobimetallic complexes which may enable (1) full catalytic cycle; (2) reactivity with external substrates.

Conflicts of interest

There are no conflicts to declare.

Acknowledgements

SG is grateful to National Science Foundation (NSF) for current support under grant number CHE-1349048. RLL thanks the NSF for computational resources (CHE-1039925 to the Midwest Undergraduate Computational Chemistry Consortium). Compound characterization was carried out at Lumigen Instrument Center at Wayne State University.

Notes and references

‡ Cu O(xanthene) distance of 2.683(2) Å appears to be too long for a bond, based on Shannon's ionic radii.[30]

1 (a) J. F. Berry, and C. M. Thomas, *Dalton Trans*., 2017, **46**, 5472-5473. (b) C. M. Thomas, *Comments Inorg. Chem*., 2011, **32**, 14-38. (c) B. G. Cooper, J. W. Napoline, and C. M. Thomas, *Cat. Rev. – Sci. Eng.*, 2012, **54**, 1-40. (d) N. P. Mankad, *Chem. Eur. J.* 2016, **22**, 5822–5829.

2 (a) S. W. Ragsdale, *Chem. Rev*., 2006, **106**, 3317-3337. (b) B. M. Hoffman, D. Lukoyanov, Z.-Y. Yang, D. R. Dean, and L. C. Seefeldt, *Chem. Rev*., 2014, **114**, 4041−4062. (c) M. Can, F. A. Armstrong, and S. W. Ragsdale, *Chem. Rev*., 2014, **114**, 4149–4174.

3 (a) H. Dobbek, L. Gremer, R. Kiefersauer, R. Huber, and O. Meyer, *Proc. Natl. Acad. Sci. U. S. A*., 2002, **99**, 15971-15976. (b) M. Gnida, R. Ferner, L. Gremer, O. Meyer, and W. Meyer-Klaucke, *Biochemistry*, 2003, **42**, 222–230.

4 R. Hille, J. Hall, and P. Basu, *Chem. Rev*., 2014, **114**, 3963–4038.

5 K. Okamoto, T. Kusano, and T. Nishino, *Curr. Pharm. Des*., 2013, **19**, 2606-2614.

6 Recent study suggests that Cu(I) site is 3-coordinate, containing weakly bound water molecule that is displaced by CO: D. Rokhsana, T. A. G. Large, M. C. Dienst, M. Retegan and F. Neese, *J. Biol. Inorg Chem*., 2016, **21**, 491–499.

7 R. Hille, S. Dingwall and J. Wilcoxen, *J. Biol. Inorg Chem*., 2015, **20**, 243–251.

8 P. E. M. Siegbahn, and A. F. Shestakov, *J. Comput. Chem*., 2005, **26,** 888–898.

9 M. Hofmann, J. K. Kassube, and T. Graf, *J. Biol. Inorg. Chem.* 2005, **10**, 490–495.

10 CO coordination to Cu(I) is also supported by EPR/ENDOR studies: (a) B. Zhang, C. F. Hemann, and R. Hille, *J. Biol. Chem*., 2010, **285**, 12571–12578. (b) M. Shanmugam, J. Wilcoxen, D. Habel-Rodriguez, G. E. Cutsail, M. L. Kirk, B. M. Hoffman, and R. Hille, *J. Am. Chem. Soc*., 2013, **135**, 17775–17782.

11 B. W. Stein, and M. L. Kirk, *Chem Commun*., 2014, **50**, 1104–1106.

12 (a) C. R. Hare, I. Bernal, and H. B. Gray, *Inorg, Chem*. 1962, **1**, 831–835. (b) J. R. Winkler, and H. B. Gray, *Struct. Bonding* (Berlin) 2012, 142, 17−28.

13 Holm, R. H. *Chem. Rev*. 1987, **87**, 1401-1449.

14 For selected examples, see: (a) M. Palucki, N. S. Finney, P. J. Pospisil, M. L. Gueler, T. Ishida, and E. N. Jacobsen, *J. Am. Chem. Soc*. 1998, **120**, 948−954. (b) D. E. Over, S. C. Critchlow, J. M. Mayer, *Inorg. Chem*. 1992, **31**, 4643−4648. (c) H. Sugimoto, S. Tatemoto, K. Toyota, K. Ashikari, M. Kubo, T. Ogurab, and S. Itoh *Chem. Commun*., 2013, **49**, 4358—4360. (d) Reynolds, M. S.; Berg, J. M.; Holm, R. H. *Inorg. Chem.* 1984, **23**, 3057−62. (e) T. A Betley, Q. Wu, Q. T. Van Voorhis, and D. G. Nocera, *Inorg. Chem*. 2008, **47**, 1849−1861. (f) J. L. Smeltz, C. P. Lilly, P. D. Boyle, and E. A. Ison, *J. Am. Chem. Soc.* 2013, **135**, 9433−9441.

15 (a) J. H. Espenson, *Coord. Chem. Rev*., 2005, **249**, 329−341. (b) Y. Wang, and J. H. Espenson, *Inorg. Chem*., 2002, **41**, 2266−2274.

16 (a) D. V. Partyka, and R. H. Holm, *Inorg. Chem*. 2004, **43**, 8609-8616. (b) D. V. Partyka, R. J. Staples, and R. H. Holm, *Inorg. Chem*. 2003, **42**, 7877-7886. (c) A. Thapper, J. P. Donahue, K. B. Musgrave, M. W. Willer, E. Nordlander, B. Hedman, K. O. Hodgson, and R. H. Holm, *Inorg. Chem*., 1999, **38**, 4104–4114. (d) J.-J. Wang, and R. H. Holm, *Inorg. Chem*. 2007, **46**, 11156-11164.

17 I. Knopf, T. Ono, M. Temprado, D. Tofan and C. C. Cummins, *Chem. Sci*., 2014, **5**, 1772-1776.

18 (a) A. Majumdar, *Dalton Trans*., 2014, **43**, 12135–12145. (b) A. Majumdar, *Dalton Trans*., 2014, *43*, 8990-9003. (c) J. S. J. Ferrara, B. Wang, E. Haas, K. W. LeBlanc, J. T. Mague, and J. P. Donahue, *Inorg. Chem.* 2016, **55**, 9173-9177.

19 (a) C. Gourlay, D. J. Nielsen, J. M. White, S. Z. Knottenbelt, M. L. Kirk, and C. G. Young, *J. Am. Chem. Soc.,* 2006, **128**, 2164–2165. (b) C. Gourlay, D. J. Nielsen, D. J. Evans, J. M. White, and C. G. Young, *Chem. Sci*., 2018, **9**, 876–888.

20 S. Groysman, A. Majumdar, S.-L. Zheng, and R. H. Holm, *Inorg. Chem.,* 2010, **49**, 1082-1089.

21 M. Takuma, Y. Ohki, and K. Tatsumi, *Inorg. Chem*., 2005, **44**, 6034-6043.

22 (a) J.-J. Wang, S. Groysman, S. C. Lee, and R. H. Holm, *J. Am. Chem. Soc.*, 2007, **129**, 7512-7513. (b) S. Groysman, J.-J. Wang, R. Tagore, S. C. Lee, and R. H. Holm*, J. Am. Chem. Soc.,* 2008, **130**, 12794-12807.

23 S. Groysman, and R. H. Holm, *Inorg. Chem*., 2009, **48**, 621-627.

24 For selected recent examples, see: (a) R. L. Hollingsworth, A. Bheemaraju, N. Lenca, R. L. Lord, and S. Groysman, *Dalton Trans.*, 2017, **46**, 5605-5616. (b) T. S. Hollingsworth, R. L. Hollingsworth, T. Rosen, and S. Groysman, *RSC Adv.*, 2017, *7,* 41819-41829.
25 R. H. Holm, E. I. Solomon, A. Majumdar, and A. Tenderholt, *Coord. Chem. Rev*. 2011, **255**, 993-1015.
26 F. A. Cotton, J. P. Donahue, and C. A. Murillo, *Inorg. Chem.*, 2001, **40**, 2229–2233.
27 J. Feng, X.-M. Lu, G. Wang, S.-Z. Du, and Y.-F. Cheng, *Dalton Trans*., 2012, 41, 8697-8702.
28 (a) R. Hille, and T. Nishino, *FASEB J*. 1995, **9**, 995–1003. (b) R. Hille, and H. Sprecher *J. Biol. Chem.* 1987, **262**, 10914–10917 (c) R. Hille, *Metal Ions in Life Sciences* 2009, **6**, 395-416.
29 C. J. Doonan, A. Stockert, R. Hille, and G. N. George, *J. Am. Chem. Soc.* 2005, **127**, 4518–4522.
30 R. D. Shannon, *Acta Cryst*. 1976, **A32**, 751-767.

Modeling the reactivity of Mo-Cu CODH: Cu(I) brings the substrate close to Mo-oxo and develops electrophilic character in CO carbon